Extension of the Certain Generalized Stresses Method for the stochastic analysis of homogeneous and laminated shells

Mahyunirsyah Mahjudin, Pascal Lardeur, Frédéric Druesne, Irwan Katili

Version of Record: https://www.sciencedirect.com/science/article/pii/S0045782520301286
Manuscript_9780ada010e9621bbe4c24abe9f2245b

Extension of the Certain Generalized Stresses Method for the stochastic analysis of homogeneous and laminated shells

Mahyunirsyah MAHJUDIN[1,2], Pascal LARDEUR[1], Frédéric DRUESNE [1], Irwan KATILI[3]

[1] Sorbonne Universités, Université de Technologie de Compiègne, CNRS FRE2012, Laboratoire Roberval, 60203 Compiègne, France
[2] Department of Civil Engineering, Institut Teknologi Medan, Medan 20217, Indonesia
[3] Department of Civil Engineering, Universitas Indonesia, Depok 16424, Indonesia
E-mail: pascal.lardeur@utc.fr

Abstract – The paper presents an extension of the Certain Generalized Stresses Method (CGSM) for the static finite element analysis of homogeneous and laminated shells with variability. The basic assumption is that the generalized stresses do not depend on input parameters perturbation. The CGSM is a non-intrusive method that requires only one finite element analysis with some load cases to calculate the variability of mechanical quantities of interest. The uncertain input parameters are material and physical properties. Uniform random parameters as well as random fields are considered. The displacements statistical results: mean value, standard deviation and distribution are obtained by Monte Carlo simulations, using a semi-analytical formula. Two examples are treated: the Scordelis-Lo shell roof and an automotive windscreen. The method provides results of good quality and is very economical from a computational time point of view.

Keywords: stochastic, finite elements, shells, laminated structures, CGSM, Monte Carlo simulation

1. Introduction

Improvement of the predictive capability of numerical models due to uncertainty is currently a relevant challenge. Taking into account uncertainty, leading to stochastic finite element models, is one way to describe more closely the physical phenomena and so to increase this predictive capability, as stated by Oberkampf et al. [1] in a paper dedicated to the verification and validation methodology. Recently much research has been carried out to develop different approaches and apply them in the context of structural mechanics. As it is well known, stochastic finite element models are usually classified in two categories: probabilistic approaches and possibilistic ones. In a probabilistic approach the input parameters are described by statistical distributions and the objective is to predict the statistics of output quantities. In possibilistic approaches, only the bounds of input parameters are defined and the objective is to calculate the bounds of the output quantities.

Taking into account uncertainty in finite element analysis of plate and shell structures, is currently a research issue. With regard to bending plates, a lot of methods have been developed, since the early contribution of Graham and Deodatis [2]. In particular for laminated plates, numerous approaches for various applications were developed, namely by Jeong and Shenoi [3],

António and Hoffbauer [4], Onkar et al. [5], Chen and Soares [6], Pandit et al. [7], Chandrashekhar and Ganguli [8], Noh and Park [9], Sobey et al. [10], Li et al. [11], Sepahvand [12], Yin et al. [13], Grover et al. [14], Tomar and Talha [15]. Argyris et al. [16] applied the weighted integral and local average methods to calculate stochastic stiffness matrices of shell structures. Then as for bending plates, stochastic analysis applied to shell structures leaded to numerous contributions. For laminated shells, Tripathi et al. [17] applied the first order perturbation technique for the free vibration stochastic analysis of laminated conical shells. Lal et al. [18] applied the perturbation technique to the geometrically nonlinear stochastic analysis of laminated cylindrical shells. Broggi and Schüeller [19] used the Monte Carlo simulation for buckling analysis of cylindrical shells. Dey et al. [20,21] and Mukhopadhyay et al. [22] used metamodels to study the stochastic natural frequencies of shells. The same type of approach was developed by Dey et al. [23] for the stochastic buckling loads of shells. Pouresmaeeli et al. [24] used the non-deterministic interval analysis method to study the variability of natural frequencies of functionally graded composite shells. Recently Tomar et al. [25] presented a state of the art of composite structures in non-deterministic framework. A lot of research contributions are cited in the paper.

Numerous research works concern the modeling of input variability parameters. Techniques and methods have been developed for the calculation of random variables and especially for random fields. First a probabilistic approach requires the choice of statistical laws. Numerous laws have been debated in the literature and used for applications. The Gaussian distribution is probably the most commonly used model for random phenomena. To prevent mathematical difficulties due to possible extreme values, truncated Gaussian laws are often used. In the context of random fields, several variants were developed for the calculation of the covariance matrix. One distinguishes between point discretization methods and average discretization ones. The well-known point methods are the midpoint method (Der Kiureghian and Ke [26]), the shape function or interpolation method (Liu et al. [27,28]), the integration point method (Brenner and Bucher [29]), the optimal linear estimation method (Li and Der Kiureghian [30]). The average methods are the local average method (Vanmarcke et al. [31,32]) and the weighted integral method (Deodatis [33], Deodatis and Shinozuka [34]). Random fields are generally represented by series discretization methods. Several approaches have been used for stochastic analysis: the singular value decomposition (Gerbrands [35]), the Karhunen-Loève expansion (Loève [36], Ghanem and Spanos [37]), the spectral representation (Shinozuka and Deodatis [38], Grigoriu [39]), and the polynomial chaos expansion (Wiener [40], Sakamoto and Ghanem [41]).

However, these existing methods have some limitations, in particular in the context of industrial applications. They are often very costly in computational time, some of them work well only if a limited number of random parameters is considered, some methods are valid only for low level variability. For industrial applications, it is important to propose non-intrusive approaches so that standard software (Abaqus, MSC/Nastran, Ansys…) can still be used. So developing an economical and reliable method accounting for the variability in the finite element calculations is still a challenge. In 2012, Lardeur et al. [42] propose the Certain Generalized Stresses Method (CGSM) for the probabilistic analysis of isotropic bars and beams. Mahjudin et al. [43] and Yin et al. [13] develop this method for homogenous plates and laminated composite plates respectively.

In this paper, the CGSM is developed for homogeneous and laminated shells with uncertain material and physical properties. These uncertain parameters are represented by random

variables or random fields. In Section 2, after recalling the principle of the CGSM, the formulation is detailed for homogeneous and laminated shells. In Section 3, two examples with several variants concerning the definition of random input parameters are treated. A synthesis of the performances of the CGSM in computational time is given in Section 4. Some conclusions and perspectives are drawn in Section 5. Nomenclature is given in Appendix.

2. The Certain Generalized Stresses Method

2.1. Basic ideas and principle of the CGSM

The flowchart of the CGSM is shown in Fig. 1. The CGSM is based on the assumption that the generalized stresses are independent of the uncertain parameters. This assumption is strictly met for statically determinate structures or if the perturbation due to uncertainty is uniform throughout the structure, that is to say if all the terms of the stiffness matrix are multiplied by the same coefficient. In reality mechanical structures are generally statically indeterminate and the perturbation is generally not uniform. Previous studies [13,42,43] have shown that the CGSM leads to satisfactory results for bar and beam trusses as well as for homogeneous or laminated plates, even if the CGSM assumption is not exactly met. The objective of this study is to assess the relevance of the mechanical assumption described above, for shells. In this paper an error indicator is proposed in order to obtain an estimation of the possible error. Thanks to this CGSM assumption, only one finite element run with some load cases, in the nominal configuration, is necessary to calculate the generalized stresses. To calculate the variability of displacement at m nodes, as explained in detail in Section 2.2, one finite element analysis with $m+1$ load cases is needed. The displacement at a given node is evaluated using Castigliano's theorem. The derivative of the strain energy with respect to the possible force applied at the point of interest leads to a semi-analytical expression of the displacement at this point. By using this expression, a Monte Carlo simulation is performed to calculate the mean value, standard deviation and distribution of the displacement. For some types of structures [42], the mean value and the standard deviation can also be obtained analytically. The CGSM can also be used to evaluate the variability of strains, stresses and failure criteria [13]. The CGSM is a non intrusive method and it is compatible with the use of any standard finite element software. In this study, Abaqus [44] has been used to treat the examples presented in Section 3. Other examples, not presented here, have been treated with the DKMQ element [45]. In summary, the CGSM can be considered as a post-treatment of one standard finite element calculation. This is an advantage from the computational time point of view. It is worth noting that nominal analyses in Abaqus are performed with standard finite elements, without any modification of their formulation. For examples

presented in Section 3, S4R shell finite elements are used. In the CGSM approach, these nominal analyses are exploited only to calculate the generalized stresses.

Verification and validation methodology has been applied as far as possible. Validation which involves experimental results is not considered in this paper. For the verification stage, mesh convergence is studied and the number of trials chosen for Monte Carlo simulations is justified. Moreover errors due to the CGSM assumption are systematically estimated through an error indicator. These issues are discussed further in next sections of the paper.

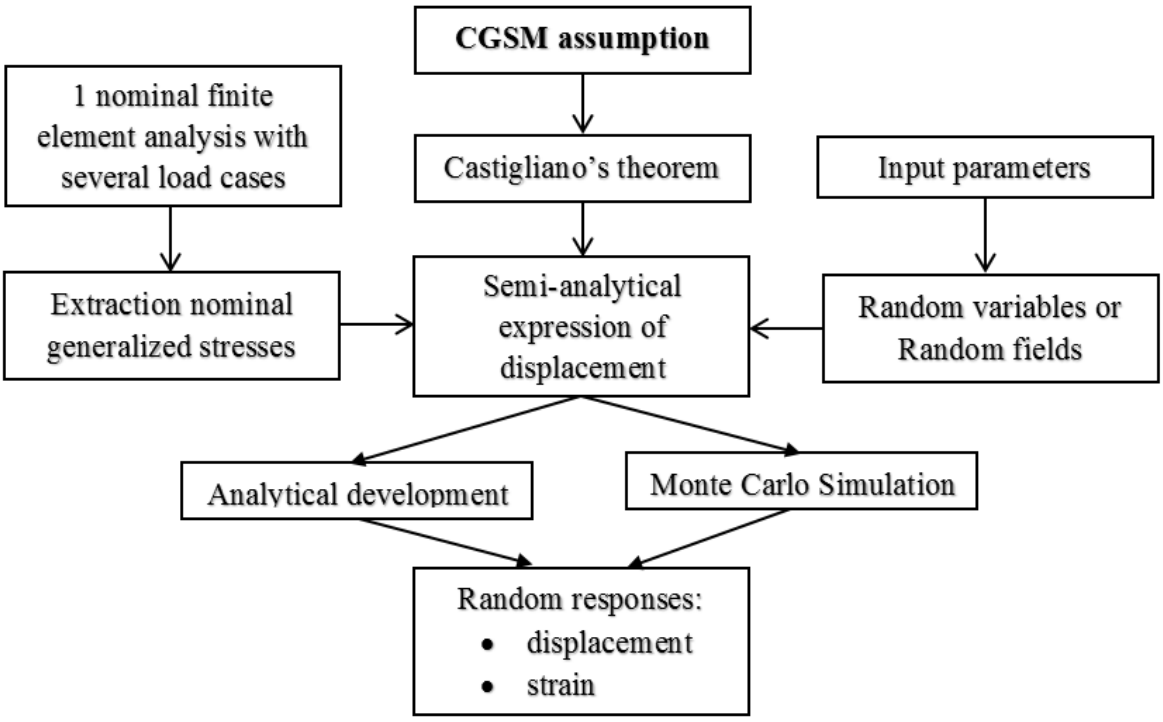

Figure 1. Principle of the CGSM method for calculating variability

2.2. Formulation of CGSM for homogeneous and laminated shells

In this section, the formulation of the CGSM is given for homogeneous and laminated shells, in particular for the calculation of the variability of displacements. This formulation takes into account material and physical properties and some of these properties may be uncertain. These uncertain parameters may be modelled by random variables or random fields. The homogeneous case being a particular case, the formulation is described only for the general laminated case. The overall strain energy is obtained by combining membrane, bending and transverse shear strain

energies. For the laminated case, it is assumed in this paper that each layer has an isotropic mechanical behavior.

The plane stress elasticity matrix for layer k is:

$$\boldsymbol{H}_k = \frac{E_k}{(1-v_k^2)}\begin{bmatrix} 1 & v_k & 0 \\ v_k & 1 & 0 \\ 0 & 0 & \frac{1-v_k}{2} \end{bmatrix} \quad \textbf{1}$$

with E_k the elasticity modulus for layer k and v_k the Poisson's ratio for layer k;

The transverse shear elasticity matrix for layer k is:

$$\boldsymbol{H}_k^s = G_k \begin{bmatrix} 1 & 0 \\ 0 & 1 \end{bmatrix} \quad \textbf{2}$$

with G_k the shear modulus for layer k.

Using the thick plate theory equations [46], the strain energy for laminated plates can be written as:

$$\pi_{int} = \frac{1}{2}\int_A \{\boldsymbol{e}\ \boldsymbol{\chi}\ \boldsymbol{\gamma}\}^T \begin{bmatrix} \boldsymbol{A} & \boldsymbol{B} & \boldsymbol{0} \\ \boldsymbol{B} & \boldsymbol{D} & \boldsymbol{0} \\ \boldsymbol{0} & \boldsymbol{0} & \boldsymbol{S} \end{bmatrix} \begin{Bmatrix} \boldsymbol{e} \\ \boldsymbol{\chi} \\ \boldsymbol{\gamma} \end{Bmatrix} dA \quad \textbf{3}$$

with $\boldsymbol{e} = \{e_x\ \ e_y\ \ e_{xy}\}^T$ the in-plane strains, $\boldsymbol{\chi} = \{\chi_x\ \ \chi_y\ \ \chi_{xy}\}^T$ the curvatures; $\boldsymbol{\gamma} = \{\gamma_{xz}\ \ \gamma_{yz}\}^T$ the out-of-plane shear strains; $\boldsymbol{A}, \boldsymbol{B}, \boldsymbol{D}$ and $\boldsymbol{S}$ the generalized membrane stiffness matrix, membrane-bending coupling stiffness matrix, bending stiffness matrix and transverse shear stiffness matrix respectively. These matrices are defined as:

$$\begin{aligned} \boldsymbol{A} &= \int_{-h/2}^{+h/2} \boldsymbol{H}_k\, dz = \sum_{k=1}^{nk} \boldsymbol{H}_k (z_{k+1} - z_k) \\ \boldsymbol{B} &= \int_{-h/2}^{+h/2} z\boldsymbol{H}_k\, dz = \frac{1}{2}\sum_{k=1}^{nk} \boldsymbol{H}_k (z_{k+1}^2 - z_k^2) \\ \boldsymbol{D} &= \int_{-h/2}^{+h/2} z^2\boldsymbol{H}_k\, dz = \frac{1}{3}\sum_{k=1}^{nk} \boldsymbol{H}_k (z_{k+1}^3 - z_k^3) \\ \boldsymbol{S} &= k^s \int_{-h/2}^{+h/2} \boldsymbol{H}_k^s\, dz = k^s \sum_{k=1}^{nk} \boldsymbol{H}_k^s (z_{k+1} - z_k) \end{aligned} \quad \textbf{4}$$

with nk the number of layers and k^s the transverse shear correction coefficient.

The relation between the strains and the generalized stresses is given by:

$$\begin{Bmatrix} \boldsymbol{e} \\ \boldsymbol{\chi} \\ \boldsymbol{\gamma} \end{Bmatrix} = \begin{bmatrix} \boldsymbol{A} & \boldsymbol{B} & \boldsymbol{0} \\ \boldsymbol{B} & \boldsymbol{D} & \boldsymbol{0} \\ \boldsymbol{0} & \boldsymbol{0} & \boldsymbol{S} \end{bmatrix}^{-1} \begin{Bmatrix} \boldsymbol{N} \\ \boldsymbol{M} \\ \boldsymbol{T} \end{Bmatrix} = \begin{bmatrix} \boldsymbol{AI} & \boldsymbol{BI} & \boldsymbol{0} \\ \boldsymbol{BI} & \boldsymbol{DI} & \boldsymbol{0} \\ \boldsymbol{0} & \boldsymbol{0} & \boldsymbol{SI} \end{bmatrix} \begin{Bmatrix} \boldsymbol{N} \\ \boldsymbol{M} \\ \boldsymbol{T} \end{Bmatrix} \quad \textbf{5}$$

with $\boldsymbol{N} = \{N_x \;\; N_y \;\; N_{xy}\}^T$ the force resultants, $\boldsymbol{M} = \{M_x \;\; M_y \;\; M_{xy}\}^T$ the bending moments and $\boldsymbol{T} = \{T_x \;\; T_y\}^T$ the transverse shear forces.

Reporting Eq. (5) into Eq. (3), one obtains:

$$\pi_{int} = \frac{1}{2}\int_A \{\boldsymbol{N} \;\; \mathbf{M} \;\; \boldsymbol{T}\}^T \begin{bmatrix} \boldsymbol{AI} & \boldsymbol{BI} & \boldsymbol{0} \\ \boldsymbol{BI} & \boldsymbol{DI} & \boldsymbol{0} \\ \boldsymbol{0} & \boldsymbol{0} & \boldsymbol{SI} \end{bmatrix} \begin{Bmatrix} \boldsymbol{N} \\ \boldsymbol{M} \\ \boldsymbol{T} \end{Bmatrix} dA \quad \textbf{6}$$

The strain energy may be decomposed into several contributions:

membrane $$\pi_{int}^{m} = \frac{1}{2}\int_A \boldsymbol{N}^T \boldsymbol{AI}\, \boldsymbol{N}\, dA \quad \textbf{7}$$

membrane-bending coupling $$\pi_{int}^{mb} = \int_A \boldsymbol{N}^T \boldsymbol{BI}\, \boldsymbol{M}\, dA \quad \textbf{8}$$

bending $$\pi_{int}^{b} = \frac{1}{2}\int_A \boldsymbol{M}^T \boldsymbol{DI}\, \boldsymbol{M}\, dA \quad \textbf{9}$$

transverse shear $$\pi_{int}^{tsh} = \frac{1}{2}\int_A \boldsymbol{T}^T \boldsymbol{SI}\, \boldsymbol{T}\, dA \quad \textbf{10}$$

Finally the strain energy can be written:

$$\pi_{int} = \frac{1}{2}\int_A \boldsymbol{N}^T \boldsymbol{AI}\, \boldsymbol{N}\; dA + \int_A \boldsymbol{N}^T\, \boldsymbol{BI}\, \boldsymbol{M}\; dA + \frac{1}{2}\int_A \boldsymbol{M}^T\, \boldsymbol{DI}\, \boldsymbol{M}\; dA + \frac{1}{2}\int_A \boldsymbol{T}^T \boldsymbol{SI}\, \boldsymbol{T}\; dA \quad \textbf{11}$$

Considering that the domain is spatially discretized and the mesh contains *n* finite elements, Eq. (11) gives:

$$\pi_{int} = \frac{1}{2}\sum_{i=1}^{n}\int_{A_i} (\boldsymbol{N}^T \boldsymbol{AI}\, \boldsymbol{N} + 2\boldsymbol{N}^T\, \boldsymbol{BI}\, \boldsymbol{M} + \boldsymbol{M}^T\, \boldsymbol{DI}\, \boldsymbol{M} + \boldsymbol{T}^T\, \boldsymbol{SI}\, \boldsymbol{T})\; dA \quad \textbf{12}$$

In order to apply the Castigliano's theorem for calculating the displacement *U* at a point *P* in a given direction, the forces in each element are decomposed into two contributions:

for the force resultants $$N_{x_i} = N_{x_i}' + F N_{x_i}'' \quad \textbf{13}$$

$$N_{y_i} = N_{y_i}' + FN_{y_i}''$$
$$N_{xy_i} = N_{xy_i}' + FN_{xy_i}''$$

for the moments

$$M_{x_i} = M_{x_i}' + FM_{x_i}''$$
$$M_{y_i} = M_{y_i}' + FM_{y_i}''$$
$$M_{xy_i} = M_{xy_i}' + FM_{xy_i}''$$

for the transverse shear forces

$$T_{x_i} = T_{x_i}' + FT_{x_i}''$$
$$T_{y_i} = T_{y_i}' + FT_{y_i}''$$

where i is the element number; F is the load applied at point P in the direction of interest (F is a force or a moment if the variability of a displacement or a rotation must be assessed respectively); the subscripts x_i, y_i indicate the local directions; $N_{x_i}', N_{y_i}', N_{xy_i}', M_{x_i}', M_{y_i}', M_{xy_i}', T_{x_i}', T_{y_i}'$ are the generalized stresses due to loads on the whole structure except at point P in the direction of interest; $N_{x_i}'', N_{y_i}'', N_{xy_i}'', M_{x_i}'', M_{y_i}'', M_{xy_i}'', T_{x_i}'', T_{y_i}''$ are the generalized stresses due to a unitary load applied at point P in the direction of interest. This decomposition requires one finite element analysis with two load cases. The first and second load cases allow the calculation of $N_{x_i}', N_{y_i}', N_{xy_i}', M_{x_i}', M_{y_i}', M_{xy_i}', T_{x_i}', T_{y_i}'$ and $N_{x_i}'', N_{y_i}'', N_{xy_i}'', M_{x_i}'', M_{y_i}'', M_{xy_i}'', T_{x_i}'', T_{y_i}''$ respectively.

Substituting Eq. (13) into Eq. (12) gives:

$$\begin{aligned}\pi_{int} = \frac{1}{2}\sum_{i=1}^{n}\int_{A_i}\Bigg(&\begin{Bmatrix} N_{x_i}' + FN_{x_i}'' \\ N_{y_i}' + FN_{y_i}'' \\ N_{xy_i}' + FN_{xy_i}'' \end{Bmatrix}^T \begin{bmatrix} AI_{11} & AI_{12} & 0 \\ AI_{12} & AI_{22} & 0 \\ 0 & 0 & AI_{33} \end{bmatrix} \begin{Bmatrix} N_{x_i}' + FN_{x_i}'' \\ N_{y_i}' + FN_{y_i}'' \\ N_{xy_i}' + FN_{xy_i}'' \end{Bmatrix} \\ &+ 2\begin{Bmatrix} N_{x_i}' + FN_{x_i}'' \\ N_{y_i}' + FN_{y_i}'' \\ N_{xy_i}' + FN_{xy_i}'' \end{Bmatrix}^T \begin{bmatrix} BI_{11} & BI_{12} & 0 \\ BI_{12} & BI_{22} & 0 \\ 0 & 0 & BI_{33} \end{bmatrix} \begin{Bmatrix} M_{x_i}' + FM_{x_i}'' \\ M_{y_i}' + FM_{y_i}'' \\ M_{xy_i}' + FM_{xy_i}'' \end{Bmatrix} \\ &+ \begin{Bmatrix} M_{x_i}' + FM_{x_i}'' \\ M_{y_i}' + FM_{y_i}'' \\ M_{xy_i}' + FM_{xy_i}'' \end{Bmatrix}^T \begin{bmatrix} DI_{11} & DI_{12} & 0 \\ DI_{12} & DI_{22} & 0 \\ 0 & 0 & DI_{33} \end{bmatrix} \begin{Bmatrix} M_{x_i}' + FM_{x_i}'' \\ M_{y_i}' + FM_{y_i}'' \\ M_{xy_i}' + FM_{xy_i}'' \end{Bmatrix} \\ &+ \begin{Bmatrix} T_{x_i}' + FT_{x_i}'' \\ T_{y_i}' + FT_{y_i}'' \end{Bmatrix}^T \begin{bmatrix} SI_{11} & 0 \\ 0 & SI_{22} \end{bmatrix} \begin{Bmatrix} T_{x_i}' + FT_{x_i}'' \\ T_{y_i}' + FT_{y_i}'' \end{Bmatrix}\Bigg) dA\end{aligned} \qquad \textbf{14}$$

Our objective is to consider simple interpolations of generalized stresses over one element. These interpolations are independent of the initial formulation of the element, consequently the development and application of the CGSM does not require any information about the

formulation of finite elements used for the nominal analysis. For T3 and Q4 elements considered here, the generalized stresses are assumed to be constant over one element [42]. The values calculated at the center of each element are considered. The relevance of this choice, directly related to convergence characteristics, is discussed in Section 3 where examples are treated. Eq. (14) becomes:

$$\begin{aligned}\pi_{int} = \sum_{i=1}^{n} \frac{A_i}{2} \Bigg(& \begin{Bmatrix} N_{x_i}' + FN_{x_i}'' \\ N_{y_i}' + FN_{y_i}'' \\ N_{xy_i}' + FN_{xy_i}'' \end{Bmatrix}^T \begin{bmatrix} AI_{11} & AI_{12} & 0 \\ AI_{12} & AI_{22} & 0 \\ 0 & 0 & AI_{33} \end{bmatrix} \begin{Bmatrix} N_{x_i}' + FN_{x_i}'' \\ N_{y_i}' + FN_{y_i}'' \\ N_{xy_i}' + FN_{xy_i}'' \end{Bmatrix} \\ & + 2 \begin{Bmatrix} N_{x_i}' + FN_{x_i}'' \\ N_{y_i}' + FN_{y_i}'' \\ N_{xy_i}' + FN_{xy_i}'' \end{Bmatrix}^T \begin{bmatrix} BI_{11} & BI_{12} & 0 \\ BI_{12} & BI_{22} & 0 \\ 0 & 0 & BI_{33} \end{bmatrix} \begin{Bmatrix} M_{x_i}' + FM_{x_i}'' \\ M_{y_i}' + FM_{y_i}'' \\ M_{xy_i}' + FM_{xy_i}'' \end{Bmatrix} \\ & + \begin{Bmatrix} M_{x_i}' + FM_{x_i}'' \\ M_{y_i}' + FM_{y_i}'' \\ M_{xy_i}' + FM_{xy_i}'' \end{Bmatrix}^T \begin{bmatrix} DI_{11} & DI_{12} & 0 \\ DI_{12} & DI_{22} & 0 \\ 0 & 0 & DI_{33} \end{bmatrix} \begin{Bmatrix} M_{x_i}' + FM_{x_i}'' \\ M_{y_i}' + FM_{y_i}'' \\ M_{xy_i}' + FM_{xy_i}'' \end{Bmatrix} \\ & + \begin{Bmatrix} T_{x_i}' + FT_{x_i}'' \\ T_{y_i}' + FT_{y_i}'' \end{Bmatrix}^T \begin{bmatrix} SI_{11} & 0 \\ 0 & SI_{22} \end{bmatrix} \begin{Bmatrix} T_{x_i}' + FT_{x_i}'' \\ T_{y_i}' + FT_{y_i}'' \end{Bmatrix} \Bigg) \end{aligned} \quad \textbf{15}$$

To obtain the displacement at a point P in a given direction, the Castigliano's theorem is applied:

$$U = \frac{\pi_{int}}{\partial F} \quad \textbf{16}$$

The displacement contains the following contributions:

$$U = \frac{\pi_{int}^{m}}{\partial F} + \frac{\pi_{int}^{mb}}{\partial F} + \frac{\pi_{int}^{b}}{\partial F} + \frac{\pi_{int}^{tsh}}{\partial F} \quad \textbf{17}$$

or

$$U = U^m + U^{mb} + U^b + U^{tsh} \quad \textbf{18}$$

where U^m is the displacement due to the force resultants, U^{mb} is the displacement due to coupling between the membrane and bending effects, U^b is the displacement due to the bending moments, and U^{tsh} is the displacement due to the transverse shear forces.

Eq. (15) is used to calculate the different terms of the displacement. Displacement due to the force resultants is:

$$U^m = \sum_i^n \frac{A_i}{2}(AI_{11}N_i^1 + AI_{22}N_i^2 + AI_{33}N_i^3 + AI_{12}N_i^4) \quad \textbf{19}$$

where:

$$\begin{aligned} N_i^1 &= 2N_{x_i}''(N_{x_i}' + FN_{x_i}'') \\ N_i^2 &= 2N_{y_i}''(N_{y_i}' + FN_{y_i}'') \\ N_i^3 &= 2N_{xy_i}''(N_{xy_i}' + FN_{xy_i}'') \\ N_i^4 &= 2(N_{x_i}'N_{y_i}'' + N_{y_i}'N_{x_i}'' + 2FN_{x_i}''N_{y_i}'') \end{aligned} \quad \textbf{20}$$

Displacement due to coupling between the membrane and bending effects is:

$$U^{mb} = \sum_i^n A_i(BI_{11}MN_i^1 + BI_{22}MN_i^2 + BI_{33}MN_i^3 + BI_{12}MN_i^4) \quad \textbf{21}$$

where:

$$\begin{aligned} MN_i^1 &= N_{x_i}'M_{x_i}'' + N_{x_i}''M_{x_i}' + 2FN_{x_i}''M_{x_i}'' \\ MN_i^2 &= N_{y_i}'M_{y_i}'' + N_{y_i}''M_{y_i}' + 2FN_{y_i}''M_{y_i}'' \\ MN_i^3 &= N_{xy_i}'M_{xy_i}'' + N_{xy_i}''M_{xy_i}' + 2FN_{xy_i}''M_{xy_i}'' \\ MN_i^4 &= N_{y_i}'M_{x_i}'' + N_{y_i}''M_{x_i}' + 2FN_{y_i}''M_{x_i}'' + N_{x_i}'M_{y_i}'' + N_{x_i}''M_{y_i}' + 2FN_{x_i}''M_{y_i}'' \end{aligned} \quad \textbf{22}$$

Displacement due to the bending moments is:

$$U^b = \sum_i^n \frac{A_i}{2}(DI_{11}M_i^1 + DI_{22}M_i^2 + DI_{33}M_i^3 + DI_{12}M_i^4) \quad \textbf{23}$$

where:

$$\begin{aligned} M_i^1 &= 2M_{x_i}''(M_{x_i}' + FM_{x_i}'') \\ M_i^2 &= 2M_{y_i}''(M_{y_i}' + FM_{y_i}'') \\ M_i^3 &= 2M_{xy_i}''(M_{xy_i}' + FM_{xy_i}'') \\ M_i^4 &= 2(M_{x_i}'M_{y_i}'' + M_{y_i}'M_{x_i}'' + 2FM_{x_i}''M_{y_i}'') \end{aligned} \quad \textbf{24}$$

Displacement due to the transverse shear forces is:

$$U^{tsh} = \sum_{i}^{n} \frac{A_i}{2} (SI_{11} T_i^1 + SI_{22} T_i^2) \quad \textbf{25}$$

where:

$$\begin{aligned} T_i^1 &= 2T_{x_i}'' \left(T_{x_i}' + FT_{x_i}''\right) \\ T_i^2 &= 2T_{y_i}'' \left(T_{y_i}' + FT_{y_i}''\right) \end{aligned} \quad \textbf{26}$$

The expression of U summarized in Eq. (18) and detailed in Eqs. (19) to (26) is used for each trial of the Monte Carlo simulation, to calculate the displacement variability of a point of a laminated shell. For the homogeneous shell case, the general formulation presented here can be simplified. Namely it can be used by ignoring displacement component due to the membrane-bending coupling contribution U^{mb}.

During the Monte Carlo simulations using the semi-analytical formula defined by Eqs. (18) to (26), ***AI***, ***BI***, ***DI*** and ***SI*** are random matrices. All other terms, in particular those which concern generalized stresses, are certain. Consequently for a given Monte Carlo trial, instead of running a finite element analysis, using the semi-analytical formula allows the calculation of a displacement. Calculating the displacement by the semi-analytical formula is much faster than running a finite element analysis. The gain due to the use of the semi-analytical formula is quantified in Section 4.

The decomposition of the generalized stresses described in Eq. (13) is specific to one given point. So, to calculate the variability of displacement at *m* nodes, one finite element analysis with *m+1* load cases is needed. This finite element analysis is performed in the nominal configuration, so for the different load cases the stiffness matrix is always the same and consequently, this matrix has to be inverted only once.

It is worth noting that the CGSM does not use any assumption concerning loading. So this method is compatible with any type of load case, namely concentrated and distributed loads may be considered. As far as linear quasi-static analysis is used, time-varying load vector may be considered as well, if the components of the load vector vary proportionally. Indeed in this case the generalized stresses vary proportionally in the same way.

2.3. Uncertainty modeling

Uncertainty modeling is represented by random variables or random fields. In Section 3, two examples are presented. The first one (Section 3.1) is studied using random fields but in the second one, only random variables are used. The uncertain input parameters are the material (E, ν) and physical (h) properties. For random fields, a specific methodology must be applied to define the values of uncertain parameters in each finite element. The CGSM is compatible with different methods for the construction of random fields. First the covariance matrix must be calculated. For the application of the CGSM to composite plates, Yin et al. [13] used the midpoint method and the local average method. For the example described in Section 3.1, the

midpoint method proposed by Der Kiureghian and Ke [26] is used. The random field is discretized at the centers of gravity of elements. The covariance matrix is defined by:

$$[COV]_{ij} = \sigma^2(1-\zeta)\exp(-\zeta) \quad \textbf{27}$$

with

$$\zeta = \frac{\Delta X_{ij}{}^2 + \Delta Y_{ij}{}^2}{\lambda^2} \quad \textbf{28}$$

where $\Delta X_{ij}$and ΔY_{ij} are respectively the distances between the midpoints of elements *i* and *j* in the *x* and *y* direction, λ is the correlation length.

Then according to Ghanem and Spanos [37], the random field is calculated by the Karhunen-Loève expansion.

2.4. Influence of the spatial discretization

Spatial discretization is an important issue in the finite element analysis of structures, particularly in presence of uncertainties. As suggested and tested by Mahjudin et al. [43], in this study it is assumed that an optimal mesh for the nominal calculation is also convenient for the variability evaluation. Therefore, the strategy adopted here is finding the optimal mesh for the nominal configuration and then exploit it to calculate the variability. The optimal mesh is identified thanks to a classical convergence study by increasing progressively the mesh refinement level.

2.5. Error indicator

Since the CGSM uses a mechanical assumption, it is important to quantify the possible errors due to this assumption. The CGSM can be validated by comparing statistical results with the direct Monte Carlo simulation, considered as the reference method. But the cost of direct Monte Carlo simulation is very high because a great number of finite element analyses is required for this method. The proposal of an error indicator for the CGSM is therefore interesting. The objective of the indicator is to quickly estimate the error level on statistical results obtained by the CGSM, compared with the direct Monte Carlo simulation. The error indicator proposed here is based on an approach proposed by Yin et al. [47] requiring a small number of random trials.

The errors between the results obtained by the CGSM and the direct Monte Carlo simulation, for a large number of trials meeting the convergence condition, are considered as the reference errors. For a number of trials *nt* the error between the MSP and the direct Monte Carlo simulation is evaluated by:

$$Err^{nt} = \frac{R^{nt}_{CGSM} - R^{nt}_{dMC}}{R^{nt}_{dMC}} \quad \textbf{29}$$

where R^{nt}_{CGSM} and R^{nt}_{dMC} are respectively the results obtained by the CGSM and the direct Monte Carlo simulation with nt trials using the same input data. These results can be the mean value, standard deviation or coefficient of variation of displacements. The objective is to verify that the errors evaluated with a small or large number (10000 trials are considered here, this number being generally considered as relevant for a good convergence level of a Monte Carlo

simulation) of trials are close. Yin et al. [47] showed that using 10 trials, the estimation of errors is quite acceptable. This error indicator is assessed in Section 3 for the two examples described.

3. Examples

3.1. Scordelis-Lo shell roof

3.1.1. Presentation of the example

The first example, presented in Figure 2, is the homogeneous and isotropic Scordelis-Lo shell roof. This example has already been treated by Stefanou and Papadrakakis [48]**.** The two longitudinal edges are free and the two circular edges are supported by rigid diaphragms. Along the rigid diaphragms it is assumed that the displacements in directions x, y, and z are zero. The roof is subjected to gravity loading with magnitude 4000 N/m^2. The geometric characteristics are: L = 15.2 m, R = 7.6 m, $\theta = 40^o$. Sensitivity study leads to the conclusion that the Poisson's ratio has no significant influence on the variability of displacements. Consequently the Poisson's ratio ν is deterministic and its value is 0.3. The random parameters are the elasticity modulus E and the thickness h, represented by isotropic random fields. Gaussian distributions are considered for E and h. As suggested by Stefanou and Papadrakakis [48], samples with non-physical parameter values are discarded. The mean values of these parameters are $m(E) = 2.1\text{x}10^{11}$ N/m^2 and $m(h)$ = 0.76 m. The coefficients of variation $CV(E)$ and $CV(h)$ are equal to 10%. An isotropic exponential correlation function defined in Eq. (27) and several correlation lengths: $\lambda = 0.004L$ to $8.55L$, are considered. The random fields are applied on the whole structure. The direct Monte Carlo simulations and the CGSM are performed with 10000 trials. The vertical displacement variability at point C, located at the middle of the longitudinal edge, is calculated.

The results of the convergence study performed in the nominal configuration are reported in Table 1. In order to show a first validation in the nominal case, the results of a classical analysis with Abaqus are given, as well as the results obtained with the CGSM formulation (Eq. (18)). In the latter case first one Abaqus analysis has been necessary to extract the generalized stresses. It is considered here that a given mesh is satisfactory if the error compared to a reference mesh is less than 0.5%. One can observe that the convergence speed is similar for a classical analysis with Abaqus and for the CGSM. This is a hopeful performance of CGSM. For this example, these results justify the choice of the approximation made in Section 2.2 (Eq. (15)), considering that the generalized stresses are constant over one element. The regular 60x84 mesh, containing 5040 S4R shell finite elements (see Figure 3), which meets the convergence criterion, is exploited for the calculation of variability.

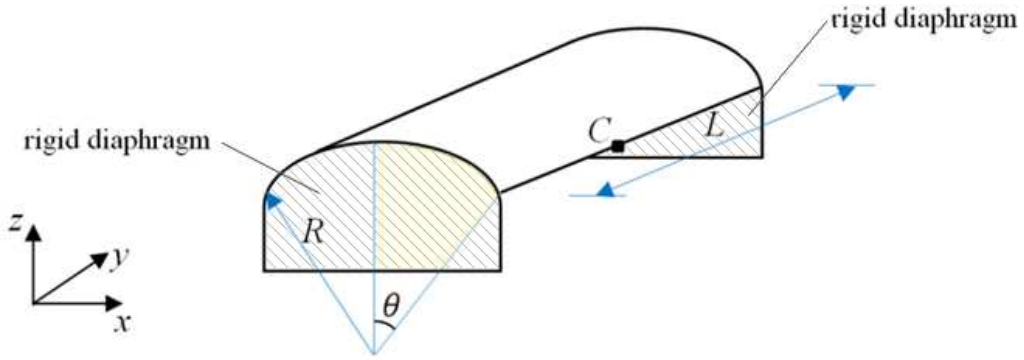

Figure 2. Scordelis-Lo shell roof under gravity loading

	Mesh 40x56 2240 elements		Mesh 60x84 5040 elements		Mesh 80x112 8960 elements
	Displacement (m)	Error (%)	Displacement (m)	Error (%)	Reference (m)
Classical FE analysis	$4.624\ 10^{-2}$	0.8	$4.596\ 10^{-2}$	0.2	$4.587\ 10^{-2}$
CGSM (Eq. (18))	$4.618\ 10^{-2}$	0.7	$4.592\ 10^{-2}$	0.1	

Table 1. Scordelis-Lo shell roof under gravity loading – convergence study of nominal displacement at node C

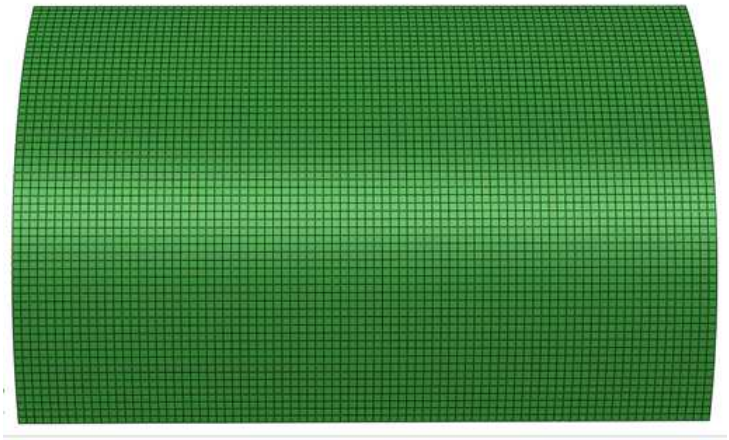

Figure 3. Scordelis-Lo shell roof under gravity loading – the 60x84 mesh (5185 nodes and 5040 S4R elements)

3.1.2. Displacement variability

The CGSM results are compared to reference solutions obtained by direct Monte Carlo simulations. In the first case, the random parameter is *E* and three correlation lengths are considered. For each correlation length, the mean value, the standard deviation and the coefficient of variation of displacement at point *C* are reported in Table 2. The mean displacement is quite stable over the whole correlation length range. However variability level of the displacement decreases for small correlation lengths. This is due to a compensation phenomenon. Errors are given in Figure 4. The errors calculated with 10000 trials as well as the values of the error estimator requiring only 10 trials are reported. The CGSM provides very

accurate results for the whole correlation length range. The errors are close to zero for a large correlation length but slightly increase when the correlation length decreases. Maximal errors are observed on the standard deviation, for the smallest correlation length case. The error estimator leads to a very good approximation of errors, indeed the difference between the error and the error estimator values is always less than 1%.

λ	$0.004L$		$0.17L$		$8.55\,L$	
	CGSM	dMC	CGSM	dMC	CGSM	dMC
$m(U)$ (m)	$4.638\ 10^{-2}$	$4.621\ 10^{-2}$	$4.639\ 10^{-2}$	$4.621\ 10^{-2}$	$4.639\ 10^{-2}$	$4.643\ 10^{-2}$
$\sigma(U)$ (m)	$1.185\ 10^{-4}$	$1.156\ 10^{-4}$	$2.029\ 10^{-4}$	$1.992\ 10^{-4}$	$4.749\ 10^{-4}$	$4.753\ 10^{-4}$
$CV(U)$ (%)	0.26	0.25	0.44	0.43	10.23	10.23

Table 2. Scordelis-Lo shell roof under gravity loading (E random, $CV(E) = 10\%$) – variability of displacement at point C

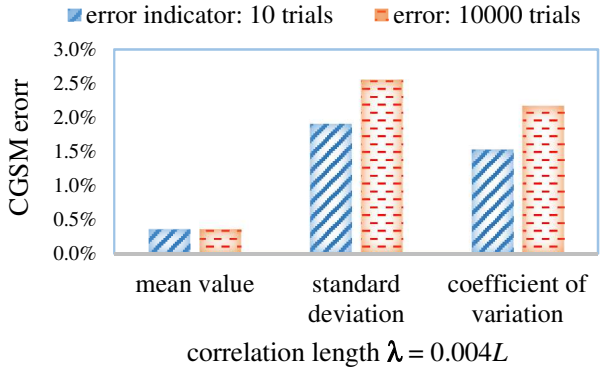

correlation length $\lambda = 0.004L$

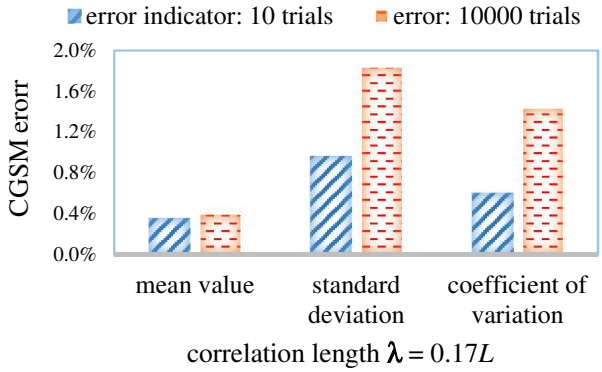

correlation length $\lambda = 0.17L$

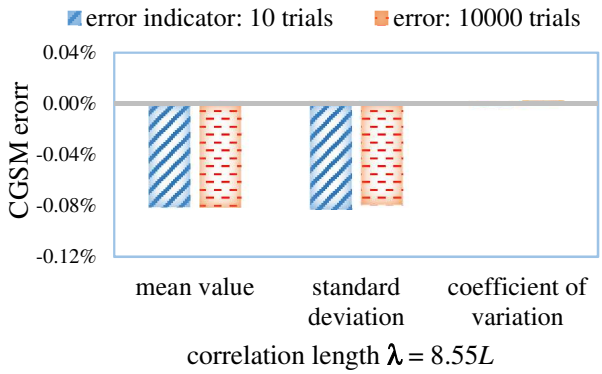

Figure 4. Scordelis-Lo shell roof under gravity loading (E random, $CV(E) = 10\%$) – errors on the statistical results of displacement at point C

In the second case, the random parameter is h and again several correlation lengths are considered. Table 3 shows the mean value, the standard deviation and the coefficient of variation of displacement obtained by the CGSM and the direct Monte Carlo simulations. Globally, the tendencies are similar to case 1, but the variability level is about twice higher when h is random. As for case 1, errors reported in Figure 5 increase for small values of the correlation length. Considering the thickness h as a random parameter leads to slightly larger errors, compared to the situation where the elasticity modulus E is random. These results show that in this example the CGSM assumption is less valid when the random parameter is the thickness. However, in all cases the errors remain acceptable, in the context of a quick method. Again, the error estimator leads to a good approximation of error, indeed the difference between the error and the error estimator values is always less than 3%.

λ	0.004L		0.17L		8.55 L	
	CGSM	dMC	CGSM	dMC	CGSM	dMC
$m(U)$ (m)	$4.754\ 10^{-2}$	$4.629\ 10^{-2}$	$4.757\ 10^{-2}$	$4.632\ 10^{-2}$	$4.756\ 10^{-2}$	$4.721\ 10^{-2}$
$\sigma(U)$ (m)	$1.585\ 10^{-4}$	$1.424\ 10^{-4}$	$4.769\ 10^{-3}$	$4.359\ 10^{-3}$	$9.934\ 10^{-3}$	$9.513\ 10^{-3}$
$CV(U)$ (%)	0.33	0.31	10.02	9.41	20.09	20.14

Table 3. Scordelis-Lo shell roof under gravity loading (h random, $CV(h) = 10\%$) – variability of displacement at point C

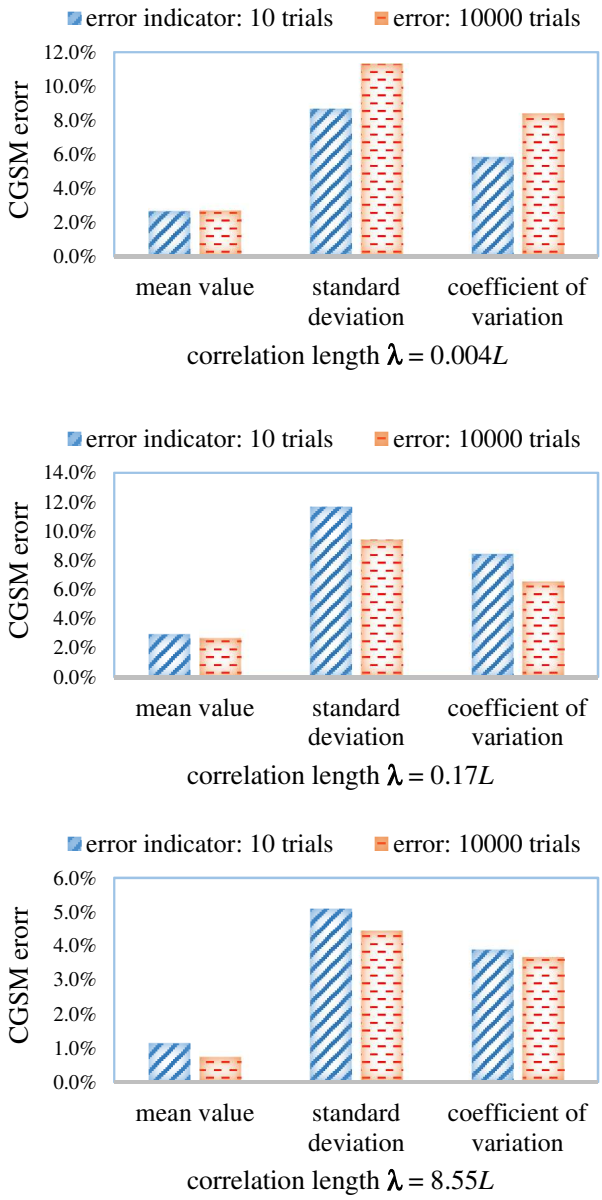

Figure 5. Scordelis-Lo shell roof under gravity loading (h random, $CV(h) = 10\%$) – errors on the statistical results of displacement at point C

Figure 6 shows the evolution of the coefficient of variation of displacement at point C, when the correlation length varies. The variability of the displacement increases non-linearly with the correlation length. For small correlation lengths, the variability level is very low. As already stated, this is due to a compensation phenomenon. This figure clearly highlights that the displacement variability level is significantly higher when the random parameter is the thickness, compared to the situation where the random parameter is the elasticity modulus. Figure 6 shows

that the CGSM, direct Monte Carlo simulation, and Stefanou and Papadrakakis [48] results are globally consistent.

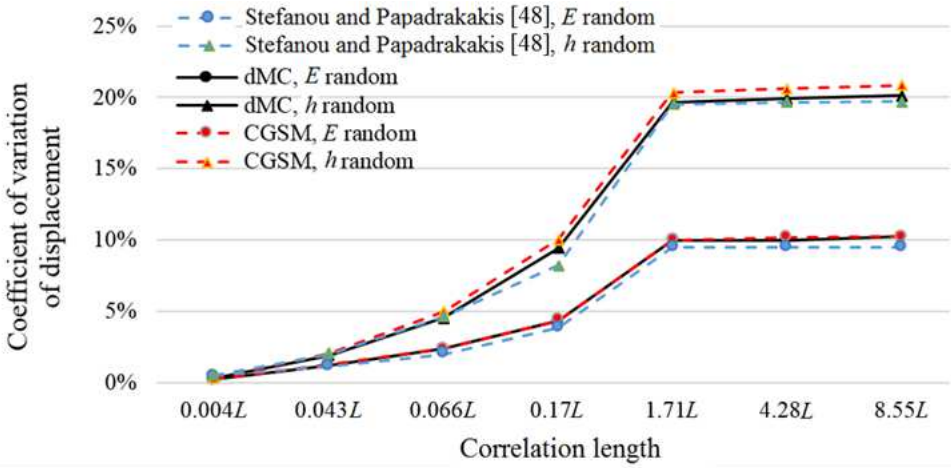

Figure 6. Scordelis-Lo shell roof under gravity loading (E or h random, $CV(E) = 10\%$, $CV(h) = 10\%$) – variability of displacement at point C

Figure 7 shows the probability density function of the displacement at point C for an intermediate correlation length value $\lambda = 0.17L$, with E or h considered as uncertain. The distributions obtained with the CGSM are very close to the reference distributions obtained with the direct Monte Carlo simulation. However, due to moderate errors when the thickness is the random parameter, some discrepancy appears in this case. The distributions are almost Gaussian.

a. E random, $CV(E) = 10\%$, $\lambda = 0.17L$

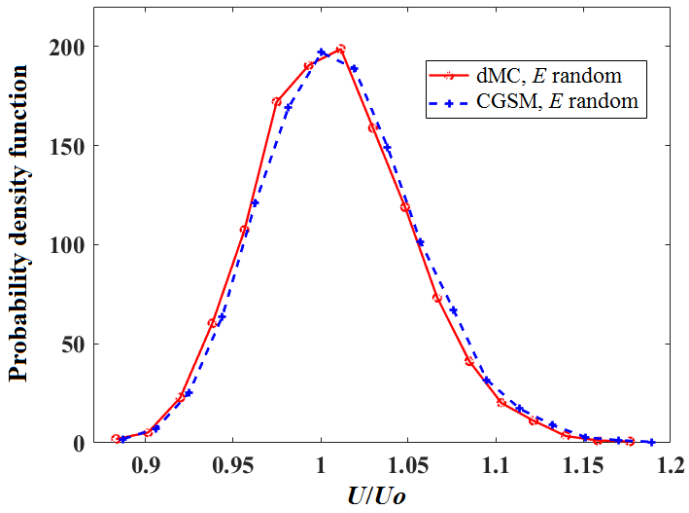

b. h random, $CV(h) = 10\%$, $\lambda = 0.17L$

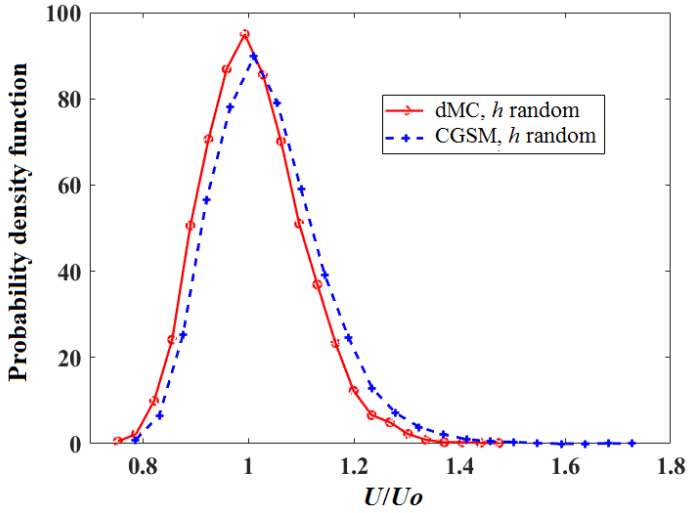

Figure 7. Scordelis-Lo shell roof under gravity loading – distribution of the displacement at point C ($U_0 = 4.592\ 10^{-2}$ m)

3.2. Windscreen

3.2.1. Presentation of the example

The second example deals with a car windscreen, which is a sandwich structure. A vibration study with variability of this Renault windscreen was presented by Scigliano et al. [49] in the context of the verification and validation methodology. This example was also treated by Arnoult et al. [50] who studied the numerical assessment of variability of natural frequencies. In the present study this structure is subjected to pressure loading with magnitude 1900 N/m^2. The windscreen is assumed clamped along its whole boundary. The sandwich structure consists of 5 layers as shown in Figure 8. The external layers (1 and 5, blue in Figure 8) are made of glass, layers 2 and 4 (yellow in Figure 8) are made of a polymer: the polyvinyl butyl (PVB). Layer 3 (orange in Figure 8) is made of a specific so-called "acoustic" polymer with very small elasticity modulus. The material properties and variability levels shown in Table 4, were initially proposed by Arnoult et al. [50], based on a study performed by the Renault company. The variability of material properties and thicknesses are represented by random variables. Truncated Gaussian distributions are considered for material properties and thicknesses, as suggested by Arnoult et al. [50]. The variables are defined for each layer and all random parameters are independent. Results are observed at point A where the displacement is maximal. The variability of the vertical displacement at point A is calculated by direct Monte Carlo simulations and the CGSM, which are both performed with 10000 trials.

The results of the convergence study in the nominal configuration are reported in Table 5. As for example 1, the values are given for a classical analysis with Abaqus, as well as for the CGSM formulation (Eq. (18)). As for the first example, one can observe that the convergence characteristics are similar for both the finite element approach and the CGSM one. These results

confirm the justification of the approximation made in Section 2.2 (Eq. (15)), considering that the generalized stresses are constant over one element. The regular mesh containing 744 S4R shell finite elements (see Figure 9), which meets the convergence criterion, is exploited for the calculation of variability.

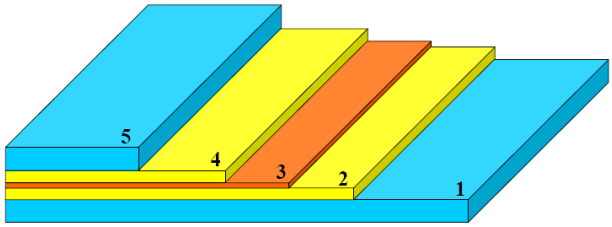

Figure 8. Car windscreen under pressure loading – stacking sequence

Layers	Elasticity modulus (MPa)	Poisson's ratio	Thickness (mm)	$CV(h_i)$ (%)	$CV(E_i)$ (%)
Glass (1)	70000	0.215	2.1	2	2
polymer PVB (2)	346	0.491	0.33	5	20
acoustic polymer (3)	12	0.491	0.1	15	20
polymer PVB (4)	346	0.491	0.33	5	20
Glass (5)	70000	0.215	2.1	2	2

Table 4. Car windscreen under pressure loading – material properties, physical properties and variability levels

	Mesh 1 192 elements		Mesh 2 744 elements		Mesh 3 13200 elements
	Displacement (mm)	Error (%)	Displacement (mm)	Error (%)	Reference (mm)
Classical FE analysis	0.1474	0.3	0.1467	0.1	0.1469
CGSM (Eq. (18))	0.1494	1.7	0.1469	0.0	

Table 5. Car windscreen under pressure loading – convergence study of nominal displacement at point *A*

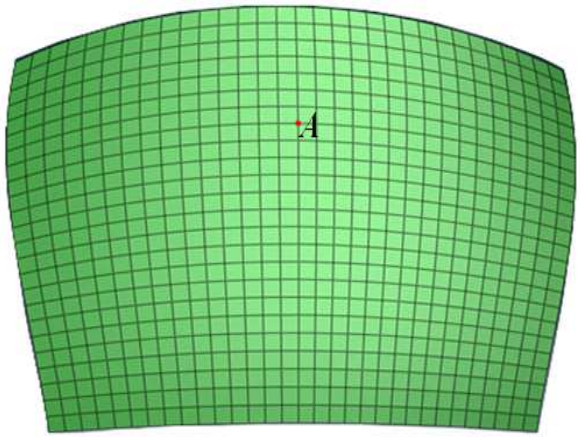

Figure 9. Car windscreen under pressure loading – finite element mesh with 744 S4R shell elements

3.2.2. Displacement variability

The CGSM results are compared to a reference solution obtained by a direct Monte Carlo simulation. Three cases are treated: the random parameters are the elasticity moduli, the thicknesses and both these two types of parameters for cases 1, 2 and 3 respectively (see Table 4). In this example there is no random field, so the parameters are uniform over a given layer. Cases 1, 2, 3 lead to 5, 5 and 10 independent random parameters respectively. For each case, the mean value, the standard deviation and the coefficient of variation of displacements at point *A* are reported in Tables 6, 7 and 8. The output variability levels are rather small. Errors are given in Figure 10. The CGSM provides very accurate results in all cases. The error estimator leads to very good approximation of errors, indeed the difference between the error and the error estimator values is always less than 2%.

.

	Random parameters: E_i	
	CGSM	dMC
$m(U)$ (mm)	0.1470	0.1468
$\sigma(U)$ (mm)	$2.014\ 10^{-3}$	$2.014\ 10^{-3}$
$CV(U)$ (%)	1.37	1.37

Table 6. Car windscreen under pressure loading (case 1: *E* random) – variability of displacement at point *A*

	Random parameters: h_i	
	CGSM	dMC
$m(U)$ (mm)	0.1470	0.1468
$\sigma(U)$ (mm)	$2.285\ 10^{-3}$	$2.282\ 10^{-3}$
$CV(U)$ (%)	1.55	1.55

Table 7. Car windscreen under pressure loading (case 2: *h* random) – variability of displacement at point *A*

	Random parameters: E_i and h_i	
	CGSM	dMC
$m(U)$ (mm)	0.1471	0.1469
$\sigma(U)$ (mm)	3.051 10^{-3}	3.049 10^{-3}
$CV(U)$ (%)	2.07	2.08

Table 8. Car windscreen under pressure loading (case 3: E and h random) – variability of displacement at point A

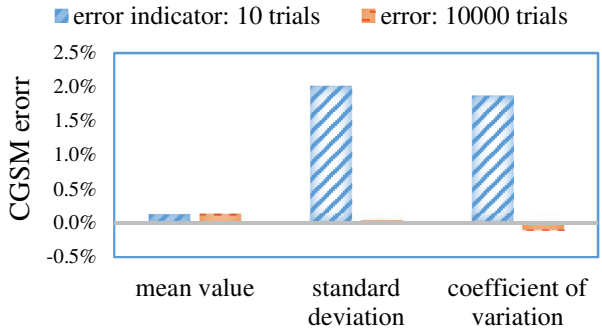

case 1: E random

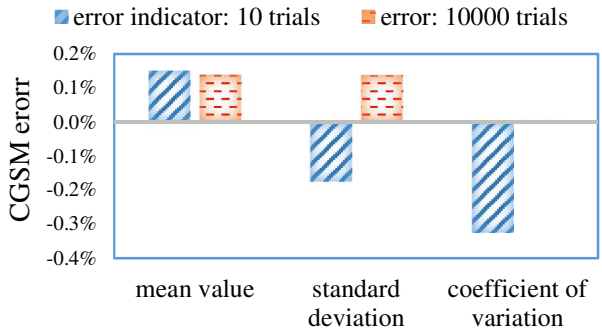

case 2: h random

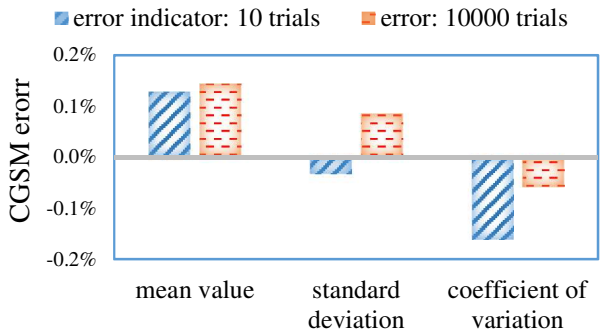

case 3: E and h random

Figure 10. Car windscreen (cases 1, 2, 3) – errors on the statistical results of displacement at point A

Figure 11 shows the probability density function of the displacement at point *A*. Again, the distribution obtained with the CGSM is very close to the reference distribution obtained with the direct Monte Carlo simulation.

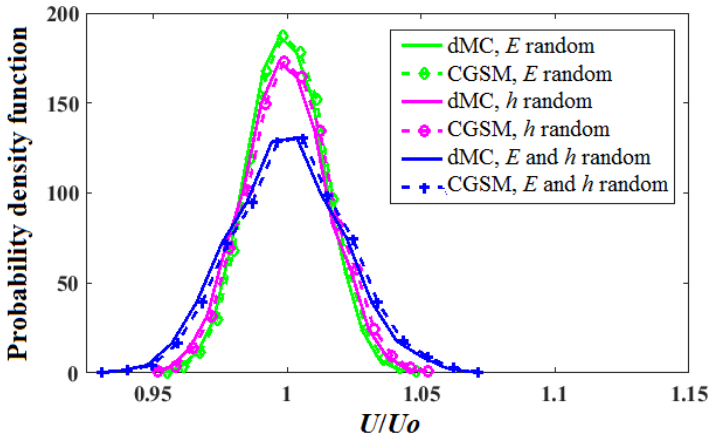

Figure 11. Car windscreen under pressure loading – distribution of displacement at point *A* (U_0 = 0.1469 mm)

In order to test the robustness of the CGSM, a complementary case, with a larger input variability level, has been treated. The elasticity moduli and the thicknesses are random. The data are identical to those reported in Table 4, except for the glass layers which have a large influence on the mechanical behavior of the windscreen. The coefficients of variation are now increased: $CV(E_i) = CV(h_i) = 10\%$ for the glass layers. Table 9 shows that the output variability level is now very high. Figure 12 shows that even in this case, errors remain quite limited and the error estimator gives satisfactory results again. Figure 13 shows the probability density function of the displacement at point *A*. Again, the distribution obtained with the CGSM is very close to the reference distribution obtained with the direct Monte Carlo simulation. These results highlight that for this example, the CGSM assumption, that is to say the generalized stresses are certain, is quite valid. The CGSM is particularly precise in this example because for one given layer, the perturbation is uniformly distributed over the whole structure. Consequently, the generalized stresses are quite certain.

	Uncertain parameters: E_i and h_i	
	CGSM	dMC
$m(U)$ (mm)	0.1494	0.1484
$\sigma(U)$ (mm)	$1.582\ 10^{-2}$	$1.560\ 10^{-2}$
$CV(U)$ (%)	10.59	10.50

Table 9. Car windscreen under pressure loading (case 4: *E* and *h* random, for glass $CV(E_i) = CV(h_i) = 10\%$) – variability of displacement at point *A*

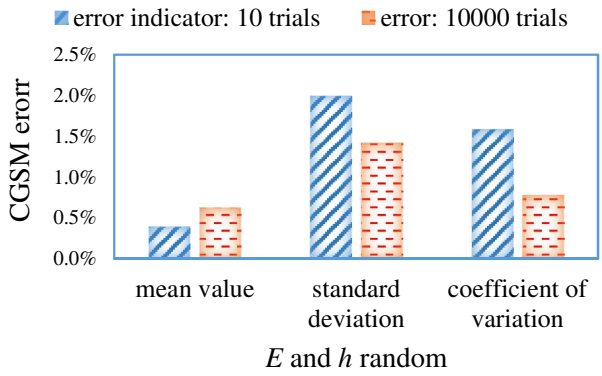

Figure 12. Car windscreen (case 4) – errors on the statistical results of displacement at point *A*

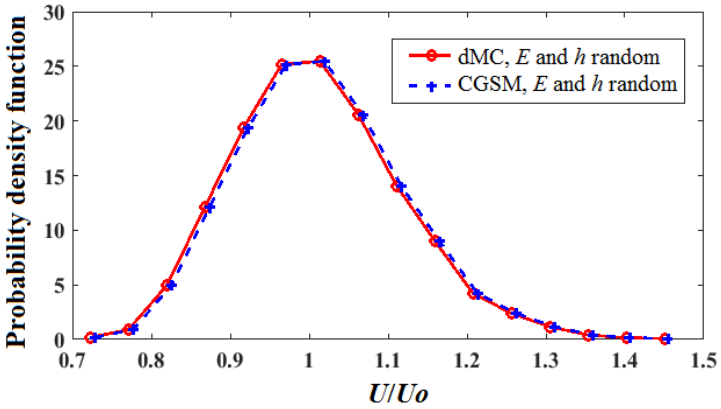

Figure 13. Car windscreen under pressure loading (case 4: *E* and *h* random, for glass $CV(E_i)$ = $CV(h_i)$ = 10%) – distribution of displacement at point *A* (U_0 = 0.1469 mm)

4. Synthesis of the performances of the CGSM in computational time

Before assessing the overall performance of the CGSM, for one trial of the Scordelis-Lo shell roof example, the net efficiency of the CGSM formula Eq. (18), compared with a classical finite element analysis, is measured. The results, presented in Table 10 for three different meshes, highlight the significant gain obtained thanks to the CGSM formula.

Mesh	CGSM formula (seconds)	Finite element analysis (seconds)	Ratio
2240 elements	$18.6\ 10^{-3}$	7.22	388
5040 elements	$5.24\ 10^{-2}$	21.6	412
8960 elements	0.124	53.5	431

Table 10. Scordelis-Lo shell roof – comparison of computational time for one trial

The tests to assess the global performance of the CGSM are performed for the industrial example: the windscreen. Results are presented in Figure 14 for several mesh refinement levels and several numbers of trials. The acceleration factor is the ratio between the total time necessary for the direct Monte Carlo simulation and the total time necessary for the CGSM. The calculation of the error indicator is taken into account in the CGSM computational time. Figure 14 shows that the acceleration factor increases with the number of trials, which is a hopeful characteristic of the method. The acceleration factor remains relatively stable for different mesh refinement levels. For a number of trials classically considered and equal to 10000, the acceleration factor is comprised between 700 and 800, depending on the mesh refinement level. This result reveals the high efficiency of the CGSM as far as computational time is concerned.

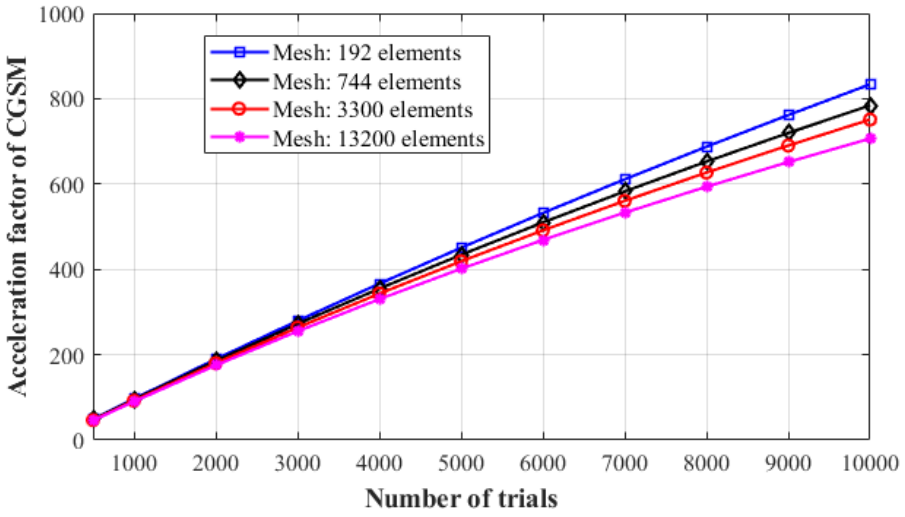

Figure 14. Car windscreen under pressure loading – acceleration factor of CGSM

5. Conclusions

This research focuses on the development and the assessment of the Certain Generalized Stresses Method for the probabilistic analysis of homogeneous and laminated shells. The variability input parameters which are elasticity moduli and thicknesses, are defined by probabilistic laws. Uniform random variables as well as random fields are considered. The outputs are statistical quantities, namely the mean value, standard deviation and probability density functions of the displacements. The CGSM statistical results are obtained by Monte Carlo simulations, using a semi-analytical formula. They are compared with the direct Monte Carlo simulation considered as a reference. An error indicator which allows calculating an estimation of the possible errors due to the CGSM assumption, is proposed. This error indicator requires 10 finite element analyses.

Two examples were treated, the Scordelis-Lo shell roof and an automotive windscreen. Satisfactory results were obtained for the mean value, the standard deviation and the probability density of displacements. In particular, the method is very powerful for the windscreen example. For both examples and different cases tested, the error estimator of statistical quantities gives satisfactory results. From a computational time point of view, the CGSM is very efficient

compared to the direct Monte Carlo simulation. The CGSM leads to a large reduction of the high computational cost that characterizes most of the existing approaches.

As a perspective, the CGSM will be assessed for laminated shells made of anisotropic materials. Other industrial cases will also be treated. For situations where the CGSM leads to some errors, it would be interesting to try and improve its efficiency. For example, the multi-fidelity concept is promising from this point of view.

Acknowledgements

The authors are grateful to the Directorate of Higher Education (DIKTI) of Ministry of Higher Education, Research and Technology of Indonesian Government and the Embassy of France in Indonesia for the financial support. The last author gratefully acknowledges research grant from Universitas Indonesia under Q1Q2 International Journal Publication Program No. NKB-0304/UN2.R3.1/HKP.05.00/2019.

References

[1] W.L. Oberkampf, T.G. Trucano, C. Hirsch. Verification, validation and predictive capability in computational engineering and physics, Applied Mechanics Reviews 57 (5), 345-384, 2004.

[2] L. Graham, G. Deodatis. Variability response functions for stochastic plate bending problems, Structural Safety, 20 (2), 167-188, 1998.

[3] H.K. Jeong, R.A. Shenoi. Probabilistic strength analysis of rectangular FRP plates using Monte Carlo simulation. Computers and Structures, 76 (1), 219-235, 2000.

[4] C.C. António, L.N. Hoffbauer. Uncertainty analysis based on sensitivity applied to angle-ply composite structures, Reliability Engineering and System Safety, 92 (10), 1353-62, 2007.

[5] A. K. Onkar, C. S. Upadhyay, D. Yadav. Probabilistic failure of laminated composite plates using the stochastic finite element method, Composite Structures, 77 (1), 79-91, 2007.

[6] N. Z. Chen, C. Guedes Soares. Spectral stochastic finite element analysis for laminated composite plates, Computer Methods in Applied Mechanics and Engineering, 197, (51–52), 4830-4839, 2008.

[7] M.K. Pandit, B.N. Singh, A.H. Sheikh. Stochastic perturbation-based finite element for deflection statistics of soft core sandwich plate with random material properties, International Journal of Mechanical Sciences, 51 (5), 363-71, 2009.

[8] M. Chandrashekhar, R. Ganguli. Nonlinear vibration analysis of composite laminated and sandwich plates with random material properties, International Journal of Mechanical Sciences, 52 (7), 874-891, 2010.

[9] H. C. Noh, T. Park. Response variability of laminate composite plates due to spatially random material parameter, Computer Methods in Applied Mechanics and Engineering, 200 (29–32), 2397-2406, 2011.

[10] A. J. Sobey, J. I. R. Blake, R. A. Shenoi. Monte Carlo reliability analysis of tophat stiffened composite plate structures under out of plane loading. Reliability Engineering and System Safety, 110, 41-49, 2013.

[11] J. Li, X. Tian, Z. Han, Y. Narita. Stochastic thermal buckling analysis of laminated plates using perturbation technique, Composite Structures, 139, 1-12, 2016.

[12] K. Sepahvand. Spectral stochastic finite element vibration analysis of fiber-reinforced composites with random fiber orientation, Composite Structures, 145, 119-128, 2016.

[13] Q. Yin, F. Druesne, P. Lardeur. The Certain Generalized Stresses Method for static analysis of multilayered composite plates with variability of material and physical properties, Composite Structures, 140, 360-368, 2016.

[14] N. Grover, R. Sahoo, B.N. Singh, D.K. Maiti. Influence of parametric uncertainties on the deflection statistics of general laminated composite and sandwich plates, Composite Structures, 171, 158-169, 2017.

[15] S. S. Tomar, M. Talha. Influence of material uncertainties on vibration and bending behaviour of skewed sandwich FGM plates, Composites part B, 163, 779-793, 2019.

[16] J. Argyris, M. Papadrakakis, G. Stefanou. Stochastic finite element analysis of shells, Computer Methods in Applied Mechanics and Engineering, 191, (41–42), 4781-4804, 2002.

[17] V. Tripathi, B.N. Singh, K.K. Shukla. Free vibration of laminated composite conical shells with random material properties. Composite Structures, 81 (1), 96-104, 2007.

[18] A. Lal, B.N. Singh, S. Kale. Stochastic post buckling analysis of laminated composite cylindrical shell panel subjected to hygrothermomechanical loading, Composite Structures, 93, 1187-1200, 2011.

[19] M. Broggi, G. I. Schuëller, Efficient modeling of imperfections for buckling analysis of composite cylindrical shells, Engineering Structures, 33 (5), 1796-1806, 2011.

[20] S. Dey, T. Mukhopadhyay, S. Adhikari. Stochastic free vibration analyses of composite shallow doubly curved shells – A Kriging model approach. Composites Part B: Engineering, 70, 99-112, 2015.

[21] S. Dey, T. Mukhopadhyay, H. Haddad Khodaparast, P. Kerfriden, S. Adhikari. Rotational and ply-level uncertainty in response of composite shallow conical shells, Composite Structures, 131, 594-605, 2015.

[22] T. Mukhopadhyay, S. Naskar, S. Dey, S. Adhikari. On quantifying the effect of noise in surrogate based stochastic free vibration analysis of laminated composite shallow shells, Composite Structures, 140, 798-805, 2016.

[23] S. Dey, T. Mukhopadhyay, S.K. Sahu, S. Adhikari. Stochastic dynamic stability analysis of composite curved panels subjected to non-uniform partial edge loading, European Journal of Mechanics A/Solids, 67, 108-122, 2018.

[24] S. Pouresmaeeli, S.A. Fazelzadeh, E. Ghavanloo, P. Marzocca. Uncertainty propagation in vibrational characteristics of functionally graded carbon nanotube-reinforced composite shell panels, International Journal of Mechanical Sciences, 149, 549-558, 2018.

[25] S. S. Tomar, S. Zafar, M. Talha, W. Gao, D. Hui. State of the art of composite structures in non-deterministic framework: A review, Thin-Walled Structures, 132, 700-716, 2018.

[26] A. Der Kiureghian, J. B. Ke, The stochastic finite element method in structural reliability, Probabilistic Engineering Mechanics, 3 (2), 83-91, 1988.

[27] W. K. Liu, T. Belytschko, A. Mani. Random field finite elements, International Journal for Numerical Methods in Engineering, 23 (10), 1831-1845, 1986.

[28] W. K. Liu, T. Belytschko, A. Mani. Probabilistic finite elements for nonlinear structural dynamics, Computer Methods in Applied Mechanics and Engineering, 56 (1), 61-81, 1986.

[29] C. E. Brenner, C. Bucher. A contribution to the SFE-based reliability assessment of nonlinear structures under dynamic loading, Probabilistic Engineering Mechanics, 10 (4), 265-273, 1995.

[30] C. Li, A. Der Kiureghian. Optimal discretization of random fields, Journal of Engineering Mechanics, 119 (6), 1136-1154, 1993.

[31] E. Vanmarcke, M. Grigoriu. Stochastic finite element analysis of simple beams, Journal of Engineering Mechanics, 109 (5), 1203-1214, 1983.

[32] E. Vanmarcke, M. Shinozuka, S. Nakagiri, G.I. Schuëller, M. Grigoriu. Random fields and stochastic finite elements, Structural Safety, 3 (3–4), 143-166, 1986.

[33] G. Deodatis. Weighted integral method. I: stochastic stiffness matrix, Journal of Engineering Mechanics, 117 (8), 1851-1864, 1991.

[34] G. Deodatis, M. Shinozuka. Weighted integral method. II: response variability and reliability, Journal of Engineering Mechanics, 117 (8), 1865–1877, 1991.

[35] J. J. Gerbrands. On the relationships between SVD, KLT and PCA, Pattern Recognition, 14 (1–6), 375-381, 1981.

[36] M. Loève. Probability theory II, Springer-Verlag, 1978.

[37] R. G. Ghanem, P. D. Spanos. Stochastic finite elements method : a spectral approach, Dover Publications, Inc, 2003.

[38] M. Shinozuka, G. Deodatis. Simulation of stochastic processes by spectral representation, Applied Mechanics Reviews, 44 (4), 191-204, 1991.

[39] M. Grigoriu. On the spectral representation method in simulation, Probabilistic Engineering Mechanics, 8 (2), 75-90, 1993.

[40] N. Wiener. The homogeneous chaos, American Journal of Mathematics, 60, 897-936, 1938.

[41] S. Sakamoto, R. Ghanem. Polynomial chaos decomposition for the simulation of non-Gaussian nonstationary stochastic processes, Journal of Engineering Mechanics, 128 (2), 190-201, 2002.

[42] P. Lardeur, É. Arnoult, L. Martini, C. Knopf-Lenoir. The Certain Generalized Stresses Method for the static finite element analysis of bar and beam trusses with variability, Finite Elements in Analysis and Design, 50, 231-242, 2012.

[43] M. Mahjudin, P. Lardeur, F. Druesne, I. Katili. Stochastic finite element analysis of plates with the Certain Generalized Stresses Method, Structural Safety, 61, 12-21, 2016.

[44] Abaqus Analysis User's Guide, Abaqus 6.14, Dassault Systèmes Simulia, 2014.

[45] I. Katili , I.J. Maknun, J.L. Batoz, A. Ibrahimbegovic. Shear deformable shell element DKMQ24 for composite structures, Composite Structures, 202, 182-200, 2018.

[46] J.N. Reddy. Mechanics of laminated composite plates and shells: theory and analysis. CRC Press; 2004.

[47] Q. Yin, F. Druesne, P. Lardeur. Performances assessment of the Modal Stability Procedure for the probabilistic free vibration analysis of laminated composite structures, Composite Structures, 203, 474-485, 2018.

[48] G. Stefanou, M. Papadrakakis. Stochastic finite element analysis of shells with combined random material and geometric properties, Computer Methods in Applied Mechanics and Engineering, 193 (1–2), 139-160, 2004.

[49] R. Scigliano, M. Scionti, P. Lardeur, Verification, validation and variability for the vibration study of a car windscreen modeled by finite elements, Finite Elements in Analysis and Design, 47, 17-29, 2011.

[50] É. Arnoult, P. Lardeur, L. Martini, The modal stability procedure for dynamic and linear finite element analysis with variability, Finite Elements in Analysis and Design, 47, 30-45, 2011.

APPENDIX: NOMENCLATURE

E_k	Young's modulus for layer k
G_k	Shear modulus for layer k
v_k	Poisson's ratio for layer k
$\boldsymbol{e}, e_x, e_y, e_{xy}$	Membrane strains
$\boldsymbol{\chi}, \chi_x, \chi_y, \chi_{xy}$	Curvatures
$\boldsymbol{\gamma}, \gamma_{xz}, \gamma_{yz}$	Transverse shear strains
$\boldsymbol{A}$	Generalized membrane stiffnesses
$\boldsymbol{B}$	Generalized membrane-bending coupling stiffnesses
$\boldsymbol{D}$	Generalized bending stiffnesses
$\boldsymbol{S}$	Generalized transverse shear stiffnesses
k^s	Transverse shear correction coefficient
nk	Number of layers
z_k	z coordinate of bottom face of layer k
h	Shell thickness
$\boldsymbol{AI}, AI_{ij}$	Generalized membrane flexibilities
$\boldsymbol{BI}, BI_{ij}$	Generalized membrane-bending coupling flexibilities
$\boldsymbol{DI}, DI_{ij}$	Generalized bending flexibilities
$\boldsymbol{SI}, SI_{ij}$	Generalized transverse shear flexibilities
A	Area of shell mid-surface
A_i	Area of shell mid-surface of element i
n	Number of finite elements
$\boldsymbol{N}, N_x, N_y, N_{xy}$	Force resultants
$N_{x_i}, N_{y_i}, N_{xy_i}$	Force resultants in element i
$N_{x_i}', N_{y_i}', N_{xy_i}'$	Force resultants in element i due to loads on the whole structure except at point P in the direction of interest
$N_{x_i}'', N_{y_i}'', N_{xy_i}''$	Force resultants in element i due to a unitary load applied at point P in the direction of interest

$\boldsymbol{M}, M_x, M_y, M_{xy}$	Bending moments
$M_{x_i}, M_{y_i}, M_{xy_i}$	Bending moments in element *i*
$M_{x_i}', M_{y_i}', M_{xy_i}'$	Bending moments in element *i* due to loads on the whole structure except at point *P* in the direction of interest
$M_{x_i}'', M_{y_i}'', M_{xy_i}''$	Bending moments in element *i* due to a unitary load applied at point *P* in the direction of interest
$\boldsymbol{T}, T_x, T_y$	Transverse shear forces
T_{x_i}, T_{y_i}	Transverse shear forces in element *i*
T_{x_i}', T_{y_i}'	Transverse shear forces in element *i* due to loads on the whole structure except at point *P* in the direction of interest
T_{x_i}'', T_{y_i}''	Transverse shear forces in element *i* due to a unitary load applied at point *P* in the direction of interest
N_i^1 to N_i^4	Defined in equation Eq. (20)
MN_i^1 to MN_i^4	Defined in equation Eq. (22)
M_i^1 to M_i^4	Defined in equation Eq. (24)
T_i^1 to T_i^2	Defined in equation Eq. (26)
π_{int}	Strain energy
π_{int}^m	Membrane strain energy
π_{int}^{mb}	Membrane-bending coupling strain energy
π_{int}^b	Bending strain energy
π_{int}^{tsh}	Transverse shear strain energy
F	Load applied at point *P* in the direction of interest
U^m	Displacement at a point *P* in a given direction due to force resultants
U^{mb}	Displacement at a point *P* in a given direction due to coupling between the membrane and bending effects
U^b	Displacement at a point *P* in a given direction due to bending moments
U^{tsh}	Displacement at a point *P* in a given direction due to transverse shear forces
$[COV]_{ij}$	Terms of the covariance matrix
ζ	Defined in Eq. (28)
ΔX_{ij}	Distance between the midpoints of elements *i* and *j* in the *x* direction
ΔY_{ij}	Distance between the midpoints of elements *i* and *j* in the *y* direction
λ	Correlation length
nt	Number of trials
Err^{nt}	Error between the results obtained by the CGSM and the direct Monte Carlo simulation for *nt* trials
R_{CGSM}^{nt}	Statistical result obtained by the CGSM with nt trials
R_{dMC}^{nt}	Statistical result obtained by the direct Monte Carlo simulation with nt trials
$m(X)$	Mean value of variable *X*

$\sigma(X)$	Standard deviation of variable X
$CV(X)$	Coefficient of variation of variable X